‘1’11(’ Effect of Rain on Nadir Ocean Backscatter in TOPEX Radar Altimeter Data

Stephen L. Durden

Jet Propulsion Laboratory, California Institute of Technology, Pasadena, CA

January 5, 1996

Rainfall profile retrieval from the 14 GHz TRMM Precipitation Radar will require correction for attenuation effects. An important technique for this is the surface reference technique, which estimates the path attenuation through rain by comparing the clear air ocean backscatter with ocean backscatter in rain. It assumes that the intrinsic ocean backscatter in the clear and raining areas is the same. There has been concern, however, that ocean backscatter in rain storms may be affected by high winds and by rainfall damping of ocean waves. We examine the effect of rain using data from the TOPEX C- and Ku band altimeter system. Results show that the intrinsic ocean backscatter within rain is typically clew to that in clear areas, supporting the use of the surface reference technique.

Corresponding Author: S.L. Durden, 818-354-4719 (ph), 818-393-5285 (fax), sdurden@jpl.nasa.gov

1 1 ntroduction

The surface reference technique (S1{'1') (Meneghini et ill. 1983; Marzoug and Amayenc 1991) has been proposed to reduce the ambiguities inherent in retrieving the rainfall profile from spaceborne radar, such as the Ku-band precipitation radar (PR) which will fly on the Tropical Rainfall Measuring Mission (TRMM) (Simpson et al., 1988). In the SRT the ocean backscatter in a clear area is compared with the ocean backscatter in the raining area, and the difference between the two yields the path integrated attenuation (I'I A), which is then used as a constraint in retrieving the rainrate profile. The SRT assumes that the intrinsic ocean cross section σ^o in the clear area and within the rain are identical. Haddad et al. (1995) showed that this assumption must be met fairly closely (<2 dB) to prevent large errors in the retrieved rain.

There has been concern that the assumption of the same σ^o in rain and clear areas may not be t'slid because of the effect of rain and wind on the ocean surface (Meneghini et al. 1992; Atlas 1994; Durden et al. 1995). In particular recent laboratory studies have noted that rain can damp ocean waves with wavelength 011 the order of 10 cm (Tsimplis 1992). This effect was noted by Atlas (1994) as large modulations of the ocean σ^o in Synthetic Aperture Radar (SAR) imagery of oceanic rain cells. The SAR imagery was acquired with incidence angles of around 20° or more, where the dominant scattering mechanism is Bragg scattering (Vesecky and Stewart 1982). The TRMM PR will operate with incidence angles between nadir and 17° where quasispecular scattering is more likely to dominate (Brown 1979; Vesecky and Stewart 1982). Because quasispecular scattering depends on the Jargc.scale surface slope variance rather than the waveheight spectrum at the Bragg wavenumber, the effect of rain damping on backscatter may be less severe near nadir than at typical SAR incidence angles. This was suggested by the results of Durden et al. (1 995), showing that the surface reference IIIA and radiometer estimated PIA near nadir were typically close to each other (1 dB RMS difference). Rain effects at nadir were also studied by Guymer et al. (1995), who presented several examples of ERS 1 altimeter measurements in rain. In most cases the backscatter in rain was reduced by attenuation; however, a few cases with enhanced backscatter, likely due to rain damping, were found.

Because of the planned TRMM launch in 1997, the possible effect of rain on ocean backscatter near nadir has some urgency. Here, it is investigated using data from the TOPEX C- and Ku-band altimeter system and the TOPEX microwave radiometer. This instrument suite allows use of two different techniques for retrieval of both the intrinsic ocean Ku-band σ^o (corrected for path attenuation) and the path averaged rain rate. We first describe the data set and analysis techniques used here and then present results of our analysis.

2 Topex Data Description and Analysis

The TOPEX/POSEIDON mission was launched in August of 1992 to study ocean circulation (Fu et al 1994). It is equipped with a radar altimeter which operates at both C-band (5.3 GHz) and a Ku-band (13.6 GHz). The altimeter is pulse limited, giving a resolution of approximately 10 km, which is about 2.5 times the expected TRMM PR footprint at nadir. TOPEX is also equipped with a microwave radiometer (18, 21, and 37 GHz), which allows path attenuation estimation and flagging of rain events. The radiometer footprint is larger than the radar resolution, ranging from 40 km at 18 GHz to 20 km at 37 GHz. We examined 8 cycles (80 days) of TOPEX GDR data from 1993 using the rain flag in the TOPEX GDR data to detect rainfall events. Data was further limited to tropical latitudes, and only data with good $\sigma 0$ values, as flagged in the TOPEX standard processing were used.

The σ^o measurements at two frequencies can be used to estimate both the intrinsic, or unattenuated σ^o, as well as the path integrated rain rate. As discussed in Olsen et al. (1978) the attenuation can be expressed as a power law of the rain rate. Our model for the σ^o measurements is

$$\sigma^o_C = \sigma^o a_C R^{1.2} + \Delta \qquad (1)$$

$$\sigma^o_{Ku} = \sigma^o - a_{Ku} R^{1.2} \qquad (2)$$

where σ^o_C and σ^o_{Ku} are the measured ocean backscatter cross sections in dB and include path attenuation effects, σ^o is the true or intrinsic backscatter cross section at Ku-band with attenuation effects removed, R is the path averaged rain rate, Δ is the clear air difference between σ^o at the two frequencies, and a is the power law constant from Olsen et al. (1978). Assuming a two way path of 10 km for tropical rain, $a_C = 0.016$ and $a_{Ku} = 0.27$. Equations (1) and (2) can be simultaneously solved to get both R and σ^o_i

$$\sigma^o = (a_{Ku}\sigma^o_C - a_C\sigma^o_{Ku} - a_{Ku}\Delta)/(a_{Ku} - a_C) \qquad (3)$$

$$R = (\sigma^o_C - \sigma^o_{Ku} - \Delta)/(a_{Ku} - a_C) \qquad (4)$$

This inversion algorithm allows us to retrieve R and σ^o from the TOPEX altimeter measurements. This approach assumes that the intrinsic σ^o at both frequencies is similarly affected by rain and wind.

The 18 GHz microwave radiometer brightness temperature can also be used to estimate path integrated attenuation (PIA) and path averaged rainfall R. To derive an algorithm for this, an Eddington approximation radiative transfer code (Kummerow 1993) was run for the model atmospheres discussed in Durden et al. (1995). These simulations included a variety of rain rates, cloud water, and surface wind conditions. Simple functions relating the Ku-band PIA (in dB) and R (in mm/h) to the 18 GHz brightness temperature were fit to the results, giving

$$PIA = 4.9 - \ln(271.7 - T_b), T_b < 271.7\text{K} \qquad (5)$$

$$R = 21.8 - 4.5 \ln(272.0 - T_b), \quad T_b < 272\text{K} \qquad (6)$$

where T_b is the 18 GHz brightness temperature. Once the PIA has been estimated, the σ^o can be estimated by adding 2 times the PIA to the measured Ku-band backscatter σ^o_{Ku}.

3 Results

Clear air measurements were used to determine that A is 3.5 dB. Measurements in rain were then processed using Equations (3) and (,1). A total of 8332 points showing the 2-frequency estimated Ku-band instrinsic backscatter cross section versus the estimated path averaged rain rate are displayed in Figure 1. The correlation coefficient is -() 05 and the slope of the regression line is -0.03. The rainrate range is from 1 to 16.4 mm/h, with a mean of 3.1 111111/11 and standard deviation of 1.8 mm/h. The intrinsic backscatter σ° ranges up to 23.5 dB, with a mean of 10.9 dB and standard deviation of 01 11% 0.95 dB. The standard deviation is close to that observed in clear conditions. The same 8332 data points were re-analyzed using Equations (5) and (6). In this case σ° is estimated by correcting the measured Ku-band backscatter (σ^o_{Ku}) by the radiometer estimated 2-way I'IA. The path averaged rain rate is also estimated from the brightness temperature. Figure 2 shows the results of this analysis, along with the linear regression line. The correlation coefficient is -0 .15 and the slope of the regression line is -0.16. The rain rate range is from 1 to 9.5 mm/h, with a mean of 1.9 mm/h and standard deviation of 1.0 mm/h. The intrinsic σ^o ranges up to 23.7 dB, with a mean of 10.8 dB and standard deviation of 1.10 dB. These results are quite similar to the results of the radar-only algorithm in Figure 1, although the rain rates are lower, likely due to partial beam filling effects in the large radiometer footprint (Graves 1993). This would also result in an underestimate of the path attenuation, making the slope of the regression line more negative than in Figure 1.

In Figure 1 the instrinsic backscatter σ^o is, on average, nearly independent of the rainrate. In Figure 2 σ^o decreases slightly, on average, with increasing rain rate. At nadir rainfall damping of waves would reduce the surface slope variance and increase σ^o. High winds in rainstorms would have the opposite effect, roughening the ocean and reducing σ^o. In both Figures 1 and 2 anomalously high and low values of σ^o can be seen. The high values could be caused by rain damping, as noted by Guymer et al. (1995), while the low values may occur in areas of very high winds. The important point here is that on the average the dependence of nadir backscatter on rain rate is small, either because the rain and wind effects are both typically small or because they often occur near each other and tend to cancel each other's effects. These results support the the underlying assumptions of the surface reference technique.

4 Conclusions

We have used TOPEX C-band and Ku-band altimeter data to retrieve both the path averaged rain rate and the intrinsic ocean surface cross section. Two algorithms were used, one using the dual-frequency radar data, the other using the Ku-band radar and 18 GHz radiometer data. A strong dependence of the intrinsic σ^o on rainfall rate was not found, possibly because the effect of rain damping on quasispecular scattering is small. Another possibilty is that smoothing of the surface due to rain often took place near areas with roughening due to wind, so that the two effects together reduced dependence of intrinsic σ^o on rain rate. The results here support the underlying assumptions of the surface reference technique.

Acknowledgment

The author would like to thank Drs. J. Martin and P. Callahan of JPL for useful discussions regarding the TOPEX instruments and data processing. The research described here was performed by the Jet Propulsion Laboratory, California Institute of Technology, under contract with the National Aeronautics and Space Administration.

References

Atlas, D. 1994, Footprints of storms on the sea - a view from spaceborne synthetic aperture radar, *J. Geophys. Res.*, 99, 796 -7969

Brown, G.S., 1979, Estimation of surface wind speeds using satellite-borne radar measurements at normal incidence, *Journal of Geophysica Research*, 84, 3974-3978.

Durden, S. L., Haddad, Z. S., Im, E., Kitiyakara, A., Li, F. K., Tanner, A. B., and Wilson, W. J., 1995, Measurement of rainfall path attenuation near nadir: A comparison of radar and radiometer methods at 3.8 GHz, *Radio Science*, 30, 943-947

Fu, ., Christiansen, E. , Yamarone, C. A., Lefebvre, M., Menard, Y., Dorrer, M., and Escudier, P., 1994, TOPEX/POSEIDON mission overview, *Journal of Geophysical Research*, 99, 24369-2438

Graves, C. E., 993, A model for the beam-filling effect associated with the microwave retrieval of rain, *J. Atmos. Oceanic Technol.*, 10, 5- 4

Guymer, T. H., Quartly, G. D., and Srokosz, M. A., 1995, The effects of rain on ERS-1 radar altimeter data, *Journal of Atmospheric and Oceanic Technology*, 12, 229-1247.

Haddad, Z. S., Jameson, A. R., Im, E., and Durden, S. ., 1995, Improved coupled Z-R and k-R relations and the resulting ambiguities in the determination of the vertical distribution of rain from the radar backscatter and the integrated attenuation *Journal of Applied Meteorlogy*, 34 268-2688

Kummerow, C., 1993, On the accuracy of the Eddington approximation for radiative transfer in the microwave frequencies, *Journal of Geophysical Research*, 98, 2757-2765.

Marzoug, M., and P. Amayenc, 1991, Improved range profiling algorithm of rainfall rate from a spaceborne radar with path-integrated attenuation constraint, *IEEE Transactions Geoscience and Remote Sensing*, 29, 584-592.

Meneghini, R., Eckerman, J., and Atlas, D., 1983, Determination of rain rate from a spaceborne radar using measurements of total attenuation, *IEEE Transactions Geoscience and Remote Sensing*, 20, 34-43.

Meneghini, R., Kozu, T., Kumagai, H., and Boncyk, W. C., 1992, A study of rain estimation methods from space using dual-wavelength radar measurements at near nadir incidence over ocean, *Journal of Atmospheric and Oceanic Technology*, 9, 364-382.

Olsen, R. L., Rodgers, D. V., and Hodge, D. B., 1978, The aR^b relation in the calculation of rain attenuation, *IEEE Transactions Antennas Propagation*, 26, 318-329.

Simpson, J., Adler, R. F., and North, G. R., 1988, A proposed tropical rainfall measuring mission (TRMM) satellite. *Bulletin American Meteorological Society*, 69, 278-295.

Tsimplis, NJ., 1992, The effect of rain in calming the sea, *Journal of Physical Oceanography*, 22.404 412.

Figure Captions

Figure   Retrieved σ^o versus ret ieved R using dual-frequency radar data and Equations (3) and (4).

Figure 2. Retrieved σ^o versus retrieved R using Ku-band radar data and 18 GHz radiometer data with Equations (5) and (6).

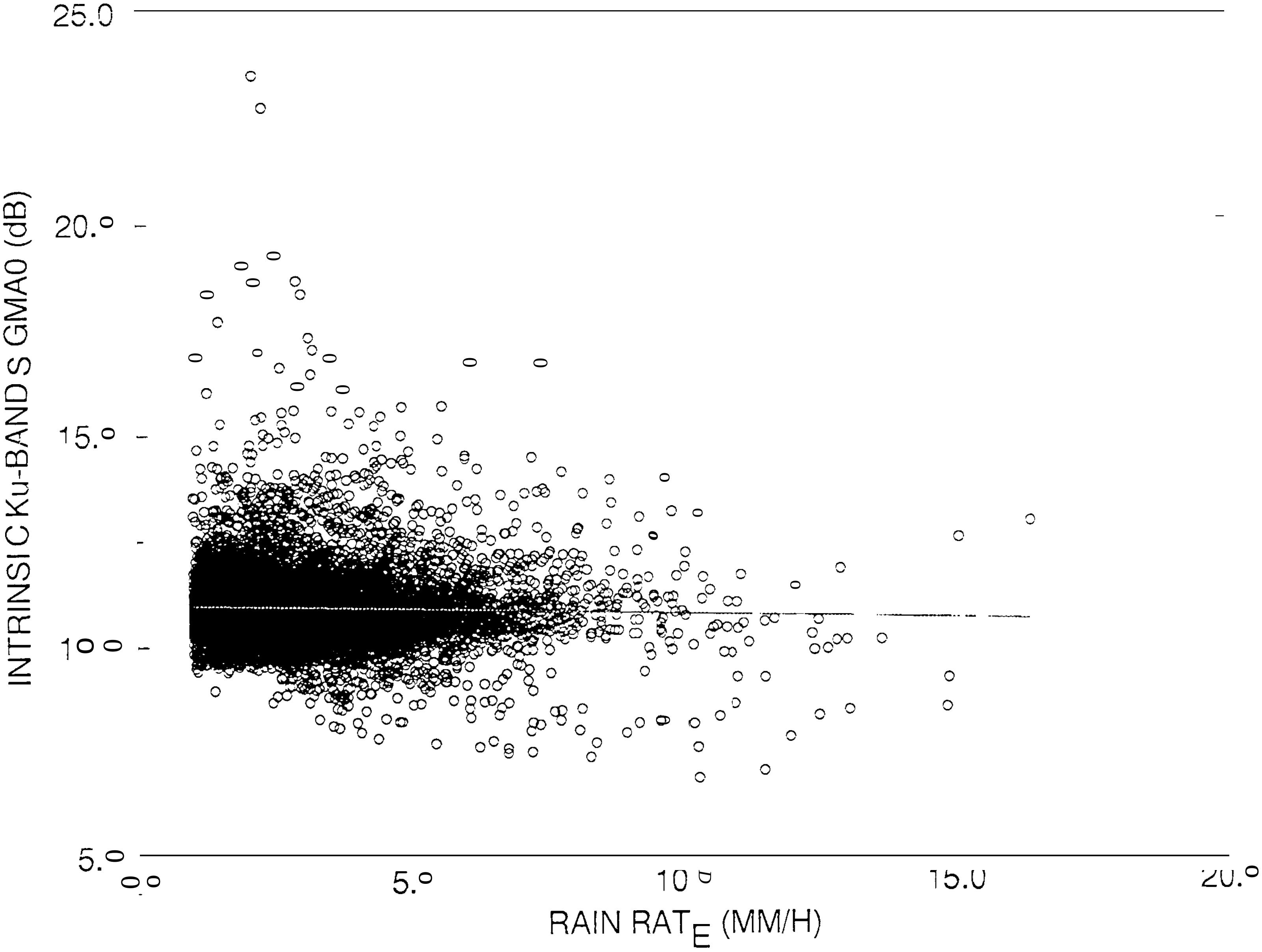
25.0
20.0
15.0
10.0
5.0
0.0
5.0
10.0
15.0
20.0
INTRINSIC Ku-BAND SIGMA0 (dB)
RAIN RATE (MM/H)

Figure 1

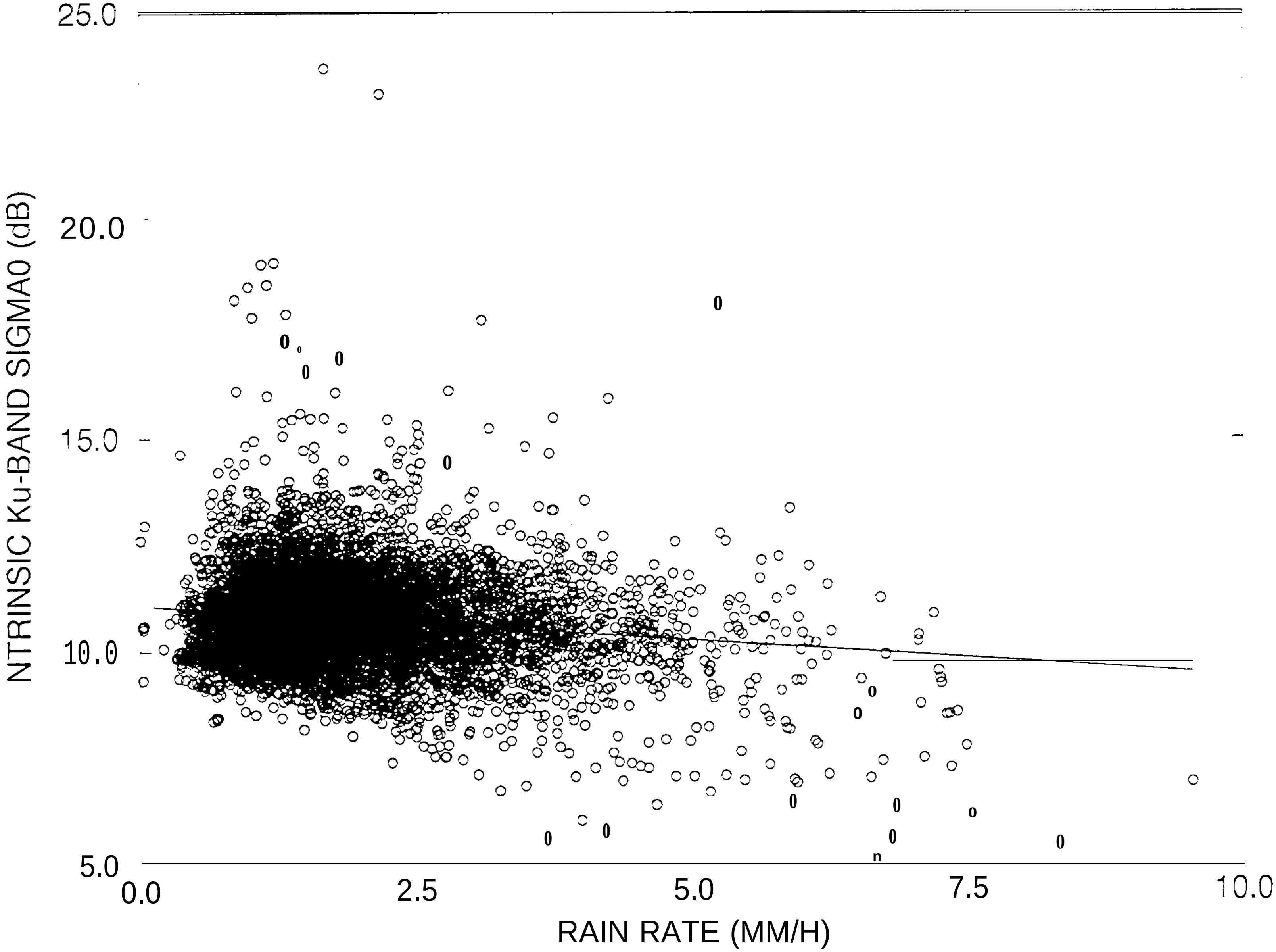

NTRINSIC Ku-BAND SIGMA0 (dB)
25.0
20.0
15.0
10.0
5.0
0.0
2.5
5.0
7.5
10.0
RAIN RATE (MM/H)

Figure 2